DRAFT SF 298

1. Report Date (dd-mm-yy)	2. Report Type	3. Dates covered (from... to)

4. Title & subtitle Yield Strength and Solution Composition Effects on Aqueous Environmental Cracking of Ti-8V-6Cr-4Zr-4Mo-3Al (Beta C) Tri-Service Committee on Corrosion Proceedings	5a. Contract or Grant #
	5b. Program Element #
6. Author(s) Biran P. Somerday Jennifer A. Grandle Richard P. Gangloff	5c. Project #
	5d. Task #
	5e. Work Unit #

7. Performing Organization Name & Address	8. Performing Organization Report #
9. Sponsoring/Monitoring Agency Name & Address Tri-Service Committee on Corrosion USAF WRIGHT-PATTERSON Air Force Base, Ohio 45433	10. Monitor Acronym
	11. Monitor Report #

12. Distribution/Availability Statement
Approved for Public Release
Distribution Unlimited

13. Supplementary Notes

14. Abstract

15. Subject Terms
Tri-Service Conference on Corrosion

Security Classification of			19. Limitation of Abstract	20. # of Pages	21. Responsible Person (Name and Telephone #)
16. Report	17. Abstract	18. This Page			

TRI-SERVICE CONFERENCE ON CORROSION

21-23 JUNE 1994

SHERATON PLAZA HOTEL
ORLANDO, FLORIDA

PROCEEDINGS

Yield Strength and Solution Composition Effects on Aqueous Environmental Cracking of Ti-8V-6Cr-4Zr-4Mo-3Al (*Beta C*)

Brian P. Somerday, Jennifer A. Grandle,
and Richard P. Gangloff

Department of Materials Science and Engineering
University of Virginia
Charlottesville, VA 22903-2442

ABSTRACT

A high-strength, α-precipitation hardened ß titanium alloy (Ti-8V-6Cr-4Zr-4Mo-3Al, STA Beta C) is prone to intergranular environmentally assisted cracking (EAC) in neutral aqueous NaCl given an occluded crack, active crack tip strain rate and electrode potential near free corrosion. The threshold stress intensity for EAC is reduced to about one-third of the plane strain fracture toughness and subcritical crack growth rates are 30 to 100 μm/sec. STA Beta C is immune to EAC with static loading or sufficiently cathodic polarization. Lower strength solution treated Beta C resists EAC in both pure NaCl and acidic sulfur-species-bearing chloride solutions, where fracture is by transgranular microvoid formation. These results are consistent with findings for STA Beta 21S and are qualitatively understood based on hydrogen environment embrittlement. EAC propagation in STA Beta C exhibits slow-rapid oscillation under rising crack mouth opening displacement but not during constant rate loading. This result implies that stress intensity factor and crack tip strain rate interactively govern da/dt.

INTRODUCTION

High-performance applications of ß titanium alloys in aggressive stress-chemical environments (e.g., geothermal brine and deep sour gas well tubulars, offshore production elements, marine fasteners, biomedical devices, and aerospace components[1]) require definition of the windows of variables that promote the aqueous environment-assisted cracking (EAC)

susceptibility of these alloys. While such investigations are extensive for α and α/ß titanium alloys,[2-5] insufficient data exist to predict EAC for body-centered cubic ß-based alloys. For titanium alloys, the challenge is complicated because EAC susceptibility is a function of test method; particularly, smooth versus cracked specimens.[3]

The objective of this research is to characterize the ambient temperature, aqueous chloride EAC behavior of a modern ß titanium alloy, Ti-3Al-8V-6Cr-4Zr-4Mo (Beta C), as a function of microstructure and/or yield strength, electrode potential, and solution composition for a single active loading rate. Precracked specimens and a fracture mechanics approach are employed. EAC susceptibility is characterized by the threshold for the onset of crack growth (K_{TH}), subcritical crack growth rate (da/dt), and the fracture mode in the aqueous environment versus the behavior in air. In addition to determining windows of variables for EAC susceptibility, these data are necessary input for damage-tolerant life prediction and fundamental studies of the crack tip damage mechanisms that govern EAC.

LITERATURE BACKGROUND

EAC of titanium alloys in aqueous halogen-bearing electrolytes is affected by several critical variables; including loading rate (crack tip strain rate), electrode potential, alloy composition, microstructure, and yield strength.

Titanium alloys, including α/ß Ti-6Al-6V-2Sn, exhibit a minimum in K_{TH} for intermediate loading rates.[6] Similar results were reported for the solution treated (ST) ß alloy Ti-13V-11Cr-3Al (VCA 120),[3] solution treated + aged (STA) ß/α Ti-11.5Mo-6Zr-4.5Sn (Beta III),[7] and modern STA ß/α Ti-15Mo-3Nb-3Al (Beta 21S).[8] STA ß/α Beta 21S and a specific age-condition of ß/α Beta III were immune to EAC under static load but susceptible under constant displacement rate deformation.[7,8] This complex loading rate dependence of EAC is unique to titanium alloys; however, some titanium alloys, including an alternate age-condition of ß/α Beta III, are susceptible to EAC under static load.[7,9]

The threshold for EAC of titanium alloys in halogenated electrolytes is generally a minimum at electrode potentials near -500 mV_{SCE}. This behavior was reported for α/ß Ti-8Al-1Mo-1V and for the ß or ß/α alloys Ti-8Mn, Beta III (STA) VCA 120 (ST), and Beta 21S (STA).[2-5,8] Immunity to EAC was achieved at cathodic potentials greater than -1000 mV_{SCE}.

The chloride EAC susceptibility of titanium alloys depends on alloy composition, microstructure, and/or yield strength (σ_{YS}). ST ß VCA 120 exhibits EAC under static loading,[10] while the ST ß alloys Beta III and Ti-

8Mo-8V-3Al-2Fe are immune. These latter two alloys become EAC-susceptible upon aging to precipitate the α phase.[3] STA β/α Beta III is susceptible to EAC under static loading for the aging condition 480°C/100 hr (σ_{YS} = 1000 MPa), but not for 620°C/16 hr (σ_{YS} = 800 MPa).[7] EAC was produced in STA β/α Beta 21S under rising displacement but not in STA β/α Ti-15V-3Cr-3Al-3Sn (Ti-15-3) for similar σ_{YS} (1300 MPa).[8] The dependence of the EAC threshold on σ_{YS} for β and β/α titanium alloys is not clear; however, limited data suggest a trend similar to that for high-strength steels.[3,5,11,12]

Sulfide additions to chloride solutions exacerbate EAC of ferritic and martensitic steels, particularly for lower strength levels.[11] Sulfide-EAC of β and β/α titanium alloys has not been investigated broadly.[13]

Considering Beta C, several studies show that this alloy is immune to chloride EAC, for the ST and STA conditions.[13-18] While smooth, notched and precracked specimens were employed, it is possible that these experiments did not sufficiently probe the intersections of the variables that cause EAC in titanium alloys.

EXPERIMENTAL PROCEDURES

Material

Beta C, of composition Ti-3.4Al-8.3V-5.9Cr-4.4Zr-4.1Mo (wt.%; with trace amounts of Nb, Fe, C, N and O as reported by the manufacturer, RMI Titanium Company) was studied. This material was provided as hot-rolled 4.1-cm diameter round bar that was solution treated above the β transus at 815°C for 1 hour followed by air cooling. EAC specimens were tested in the ST and STA conditions. The aging treatment consisted of heating ST blanks at 500°C for 24 hours followed by air cooling. This treatment precipitated α as 1 to 5 μm long platelets within 120 μm grains and infrequently in a colony structure at β grain boundaries. Transmission electron microscopy was not conducted; particularly, the occurrence of a submicron α film on β grain boundaries was not determined. Rockwell C hardnesses were R_c 28 and R_c 41 for the ST and STA conditions, respectively, which correspond to yield strengths of 830 and 1280 MPa from a hardness-σ_{YS} correlation given for two β titanium alloys.[8]

Environment

Experiments were conducted at 25°C in either moist air or neutral (pH 6) 0.6M (3.5 wt.%) aqueous NaCl at free corrosion or fixed electrode potentials of -150, -600, and -1000 mV_{SCE}. Experiments were also conducted in the acidified sulfur-species-bearing solutions indicated in Table I. A plexiglass cell was secured to the specimen in order to flow solution

at 25 ml/min from a two-liter reservoir through the machined notch tip and fatigue precrack. A schematic of the cell is shown in Fig. 1. Dissimilar metals did not contact the specimen and all tubing was PTFE. The grounded specimen (working electrode) was maintained at a constant potential by a Wenking potentiostat in conjunction with a chloridized silver wire reference electrode and a platinized niobium counter electrode. The reference electrode for polarization was located on one side of the specimen, near the notch (Fig. 1). A second reference electrode indicated that the potential of the opposite face was 0 to 200 mV more noble than the polarized side, depending on the magnitude of the current.

Table I. Sulfur-Species Additions to the Aqueous NaCl Environment

Solution	Salt	Acid / pH	Sulfur Compound	Sulfur Species
Sulfide + acetic	0.6 M NaCl	1.5M acetic, 0.1M acetate / pH 3.3	10 ppm S as Na_2S	CH_3COSH (?)
Sulfide + hydrochloric	0.6 M NaCl	0.1 M HCl pH 1.3	4 ppm S as Na_2S	H_2S
Thiosulfate + acetic	0.9 M NaCl	0.15 M acetic pH 2.6	60 ppm S as $Na_2S_2O_3$	$S_2O_3^{=} \rightarrow S \rightarrow H_2S$(?)

EAC-Fracture Mechanics

Sidegrooved compact tension (CT) specimens were machined with the longitudinal axis of the round bar perpendicular to the crack plane and crack growth in the radial direction. CT specimen gross thickness was 6.3 mm, net thickness was 5.1 mm, and width was 30.5 mm. Specimens were fatigue precracked in room temperature moist air, terminating with a K_{MAX} of 25 MPa$\sqrt{m}$, R of 0.4 ($R = K_{MIN}/K_{MAX}$), and a crack length-to-width ratio (a/W) of approximately 0.52.

Precracked specimens were loaded under monotonically rising crack mouth opening displacement (CMOD) at a constant rate ($\dot{\delta}_M$) of 1.8 μm/min using a servohydraulic mechanical test system. CT specimens were instrumented to measure applied load, CMOD and crack extension. CMOD was measured and controlled using a clip gauge mounted across the mouth of the machined notch, as shown in Fig. 1. The direct current potential difference (DCPD) method was used to resolve crack tip process zone damage initiation and subsequent crack growth. The expression used to calculate a/W from measured voltage, and other details of the technique,

are given in References 8, 19 and 22. Applied load, DCPD, CMOD and time were recorded using a PC-based data acquisition system.

The fracture mechanics were characterized using the elastic-plastic J-integral, as detailed elsewhere.[19] For STA specimens $J_{plastic}$ was small compared to the applied total J; thus small-scale yielding was maintained and elastic K analysis was sufficient. All experiments satisfied the criterion for plane strain defined in an ASTM Standard.[20]

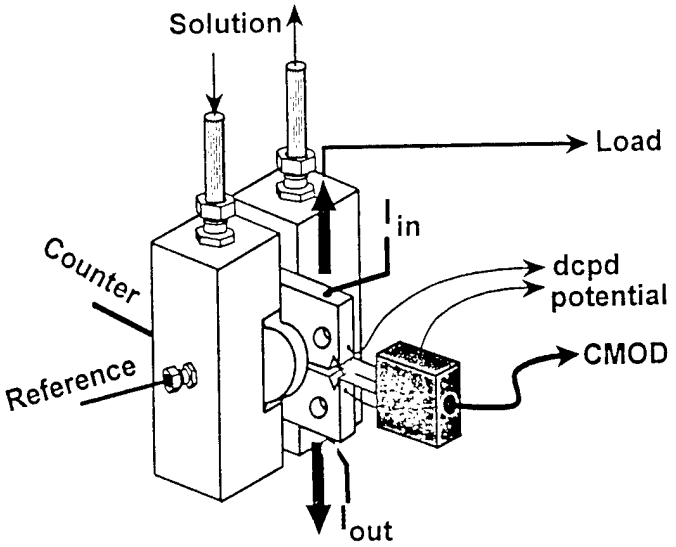

Figure 1. Cell and CT specimen for rising CMOD EAC experiments. ("dcpd" indicates the measurement probes for electrical potential difference due to a direct current, I, through the uncracked portion of the specimen.)

The plot of load and DCPD versus CMOD in Fig. 2 is typical of the experiments with high-strength STA specimens in NaCl. Two measures of the threshold K for the initiation of crack growth were determined. A lower-bound value is defined by the first deviation from the initial baseline DCPD versus CMOD trend when coincident with the onset of nonlinearity in the load versus CMOD plot.[8,19] For loading in moist air, this value (K_{ICI}) is a lower bound of the standardized plane strain fracture initiation toughness (K_{IC}),[19] and in aggressive environments this value (K_{THi}) represents a lower bound of the threshold (K_{TH}) for subcritical crack growth initiation.[21] K_{TH} is

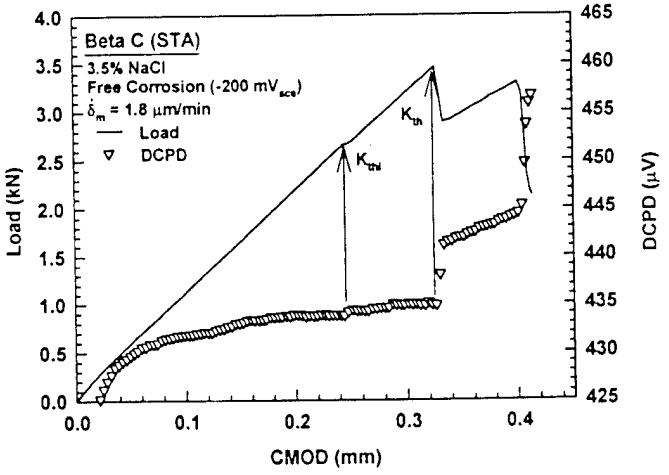

Figure 2. Load and DCPD versus CMOD data for STA Beta C in 3.5% NaCl. (Note the definition of threshold stress intensity (K_{TH}) and initiation threshold stress intensity (K_{THi}).)

defined at the first major load drop. At K_{THi}, the crack growth increment (Δa) is assumed to equal zero; subsequent crack lengths are calculated using DCPD values normalized with the potential at the known fatigue precrack length.[19,22] Average subcritical crack growth rate (da/dt) was calculated using linear regression over a small time interval.

A single critical J for the initiation of crack growth was calculated for each ST experiment since DCPD versus CMOD data did not indicate crack initiation. The initiation point was determined from DCPD measurements with the measured final crack length as a reference, then selecting the P-CMOD data point corresponding to the measured fatigue precrack length.

RESULTS

ST Beta C in Air and Chloride

Static Crack / Threshold Behavior Results for ST Beta C tested in moist air and four different aqueous environments, each at the free corrosion potential, are shown in Fig. 3. These experiments establish that Beta C in the moderate strength, single phase condition is not embrittled by severe mechanical and environmental conditions. The CMOD rate used for these experiments produced maximum EAC susceptibility (minimum K_{TH}) for STA ß/α Beta 21S in aqueous NaCl near free corrosion.[8] The moist air fracture toughness (K_{IC}) of ST Beta C is 115 MPa√m, which compares favorably with a reported value of 96 MPa√m.[23] The higher value may reflect the use of elastic-plastic fracture mechanics for small specimens of a moderate strength-high toughness alloy, compared to the less rigorous elastic analysis employed in Ref. 23. K_{TH} (114 MPa√m) in neutral NaCl (E_{corr} = -200 to -750 mV_{SCE}) was not reduced compared to K_{IC}.

The addition of sulfur species to NaCl solutions, particularly those that form hydrogen sulfide (H_2S), exacerbates EAC in steel.[24-27] In contrast Fig. 3 shows that K_{TH} (113 to 120 MPa√m) for ST Beta C in three different sulfur-species-containing aqueous media (E_{corr} ~ -250 mV_{SCE}) is not reduced compared to either K_{IC}

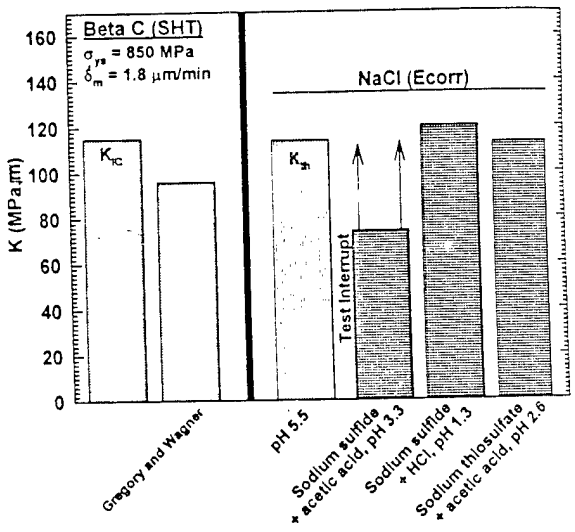

Figure 3. K_{IC} and K_{TH} data for ST Beta C. K_{IC} is for moist air, compared to the value from Ref. 23, while K_{TH} data are for the NaCl/sulfur-species solutions listed in Table I.

or K_{TH} for pure NaCl. In the Na_2S/acetic acid solution, Na_2S reacts to form thioacetic acid;[24] H_2S gas was not detected by smell. (Crack growth was not detected at the point where this experiment was terminated due to cell leakage. K_{TH} therefore exceeded the K value calculated at the test-interrupt load.) H_2S formed in the Na_2S/HCl acid solution.[25] The sodium thiosulfate/acetic acid solution forms elemental sulfur and H_2S in the presence of steel.[26]

Figure 4 shows typical scanning electron microscope (SEM) fractographs of the K_{IC} or K_{TH} regions of CT specimens of ST Beta C, fractured in moist air or acidified NaCl/Na_2S. The fracture mode is identical for moist air and all aqueous environments in Table I, and consists predominately of fine (of order 2 μm) transgranular microvoids.

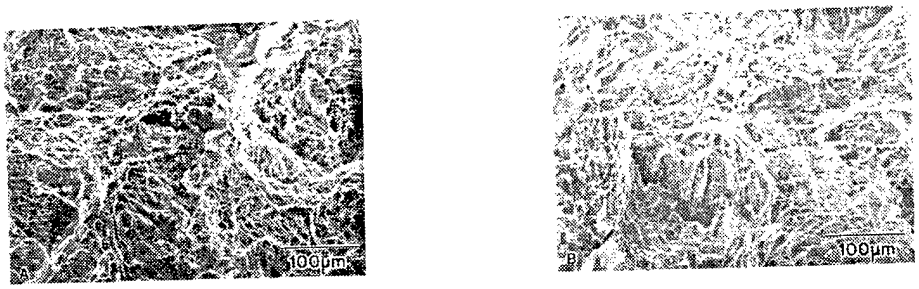

Figure 4. SEM fractographs for ST Beta C in (a) moist air and (b) acidic NaCl/Na_2S. The crack grew from top to bottom, and the fractographs are located in the central crack initiation region.

Equal K_{IC} and K_{TH}, as well as identical fracture modes in moist air and the solutions, indicates that ST Beta C is immune to EAC, at least for the loading rate and electrode potential conditions that were examined.

STA Beta C in Air and Chloride

Static Crack/Threshold Behavior Results for high-strength STA Beta C, tested in moist air and neutral aqueous NaCl at -600 mV_{SCE} and fixed δ_M, are shown in Fig. 5. Filled circles represent the results of individual experiments, while averages are given by the bars. K_{IC} is 50% lower (56 MPa$\sqrt{m}$) than for the ST condition, consistent with the substantially higher strength from aging. K_{TH} for chloride (35 MPa$\sqrt{m}$) is reduced by about one-third compared to K_{IC}. Data for STA Beta 21S and STA Ti-15-3,[8] obtained with single-edge-cracked specimens fractured in air and neutral aqueous NaCl at -600 mV_{SCE} by the same procedure as Beta C, are included in Fig. 5. The plane strain fracture toughness of STA Beta C is lower than that of the other two high-strength alloys. Similar to the behavior of Beta C, K_{TH} for

Beta 21S is reduced compared to K_{IC}. In contrast K_{TH} equals K_{IC} for Ti-15-3.

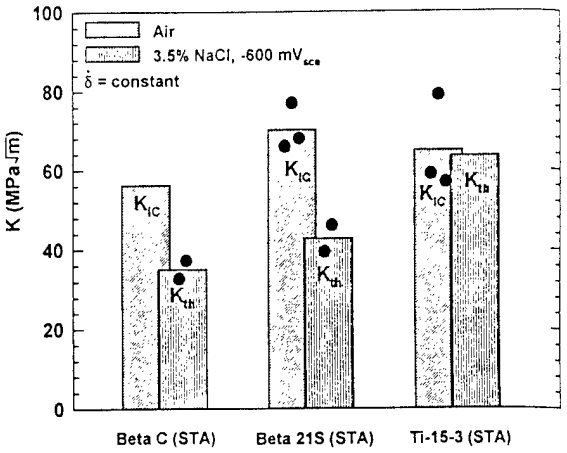

Figure 5. Rising CMOD K_{IC} and K_{TH} data for Beta C, Beta 21S[8], and Ti-15-3[8] (all STA) in air and aqueous NaCl. The bars are average values and filled circles represent individual results.

Figure 6 shows SEM fractographs from CT specimens of STA Beta C tested in moist air and aqueous NaCl. Fracture in air occurs predominately *via* transgranular microvoid coalescence. Both small (of order 2 to 5 μm) equiaxed and larger elongated microvoids are observed. Some facets are also present and may consist of fine (of order 1 μm) microvoids. Fracture occurs by intergranular separation in the chloride environment. No transition region is evident between the fatigue crack front and EAC intergranular facets. Fine void-like features are present on grain facets. The moist air fracture modes for STA Beta 21S and STA Ti-15-3[8,28] resemble that for Beta C in air. The air fracture mode was not altered for Ti-15-3 tested in aqueous NaCl, whereas Beta 21S failed by intergranular separation.[8]

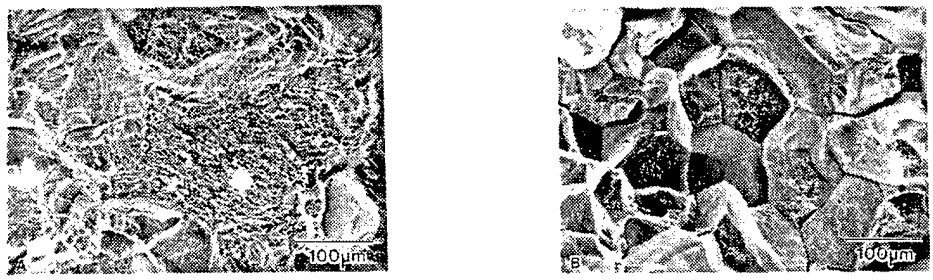

Figure 6. SEM fractographs for STA Beta C in (a) moist air and (b) 3.5% NaCl. The crack grew from top to bottom.

K_{TH} less than K_{IC}, as well as the change in fracture mode from transgranular microvoid rupture to grain boundary separation, indicates that STA Beta C is susceptible to EAC in neutral aqueous NaCl at electrode potentials near -600 mV_{SCE} and under rising CMOD.

Figure 7 shows the effect of maintaining a CT specimen of Beta C at constant CMOD in aqueous NaCl after interrupting the rising CMOD at a

K level (47 MPa√m) greater than K_{TH}. (For this experiment, the rising CMOD was interrupted during decreasing load and rapid subcritical crack propagation.) Crack propagation continued for less than one minute after CMOD was fixed. At this point, DCPD data indicate no crack growth, or at most a limiting da/dt of 0.001 μm/s over 90 hours. Crack growth-induced compliance changes were not detected (dP/dt was essentially zero over this time period), suggesting that da/dt was zero.

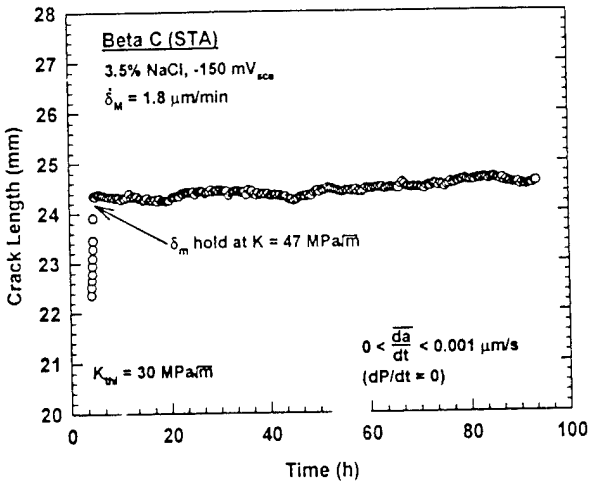

Figure 7. Crack length versus time for an experiment with STA Beta C in NaCl which was interrupted and maintained at constant CMOD (δ_M) for a K level above K_{TH}.

Potentiostatic Polarization The severity of EAC for STA Beta C in pure NaCl depends on applied electrode potential, as shown in Fig. 8. Both K_{THi} and K_{TH} are compared to K_{TH} data for Beta 21S.[8,28] EAC is observed (K_{THi} and K_{TH} are less than K_{ICi}, coupled with intergranular cracking) for applied potentials between -150 and -600 mV_{SCE}, and threshold is a minimum for a potential of -600 mV_{SCE}. At a potential of -1000 mV_{SCE}, STA Beta C is immune to EAC (K_{THi} equals K_{ICi} and fracture is by microvoid rupture for chloride and moist air). The effect of potential is similar for STA Beta 21S.

Subcritical Crack Propagation Two distinct subcritical crack propagation rate responses were observed for STA Beta C in NaCl. Figure 9 shows results for an experiment at -150 mV_{SCE}. Subcritical crack propagation was slow (on the order of 0.1 μm/s) for rising K levels just above K_{THi} (30 MPa√m). At K equal to K_{TH} (41 MPa√m), the da/dt accelerated by two orders of magnitude under decreasing K from 41 to 35 MPa√m (applied K values are indicated at several points in Fig. 9). After a crack growth increment of 2 mm, da/dt decreased abruptly to near the initial rate. This slow-fast sequence was repeated several times as the

chloride crack propagated subcritically in several EAC experiments.[1]

In contrast to the behavior in Fig. 9, alternating slow-fast da/dt was not observed for EAC experiments with STA Beta C/NaCl under rising load control. Figure 10 shows that rapid crack propagation is not arrested and continues until specimen fracture. The fast crack growth rates indicated in Figs. 9 and 10 are consistent with limited values reported for other ß-titanium alloys.[3,5,7,28] It is difficult to quantify the slower EAC rates in Fig. 10, at K just above K_{THi}. This behavior appears akin to the so-called Stage IIA behavior reported for α/ß titanium alloys in aqueous chloride.[29]

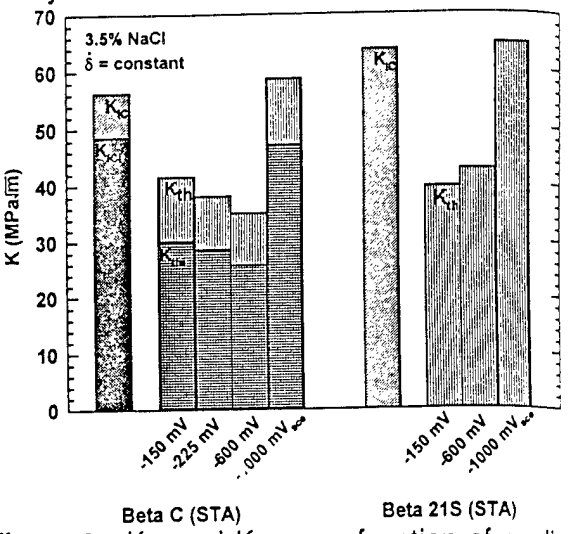

Figure 8. K_{TH} and K_{THi} as a function of applied electrode potential for STA Beta C and STA Beta 21S[8] in aqueous chloride solution. Moist air K_c is also shown.

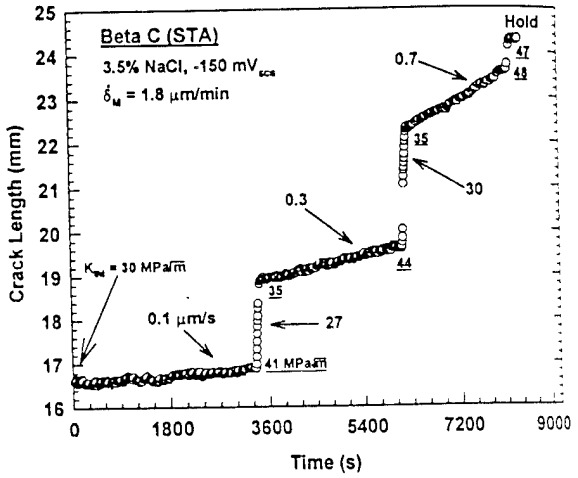

Figure 9. Crack length versus time for STA Beta C in 3.5% NaCl at -150 mV_{SCE} and constant $\dot{\delta}_M$. Average crack growth rates at various K levels (underlined) are shown.

DISCUSSION

Comparison to Literature Results for EAC of Beta C

Literature results indicate that Beta C is immune to aqueous chloride EAC.[13-18] Aylor studied ST Beta C (σ_{YS} = 850 MPa) with blunt-notched tensile specimens under rising displacement in aqueous NaCl at free corrosion and applied electrode potentials between

[1]The point marked "Hold" in Fig. 9 shows the onset of the fixed CMOD experiment shown in Fig. 7, which did not produce EAC propagation in Beta C/NaCl. Here, CMOD was fixed during a rapid da/dt event under decreasing K. A similar result (viz., no subcritical EAC propagation for 50 hours at constant CMOD and applied K greater than $K_{...}$ was observed for an experiment interrupted during slow da/dt and rising K.

-850 and -1250 mV_{SCE}.[14] These conditions did not produce EAC in Beta C. This procedure indicated that α/β Ti-6Al-4V (Ti-6-4) at this same yield strength is chloride-cracking resistant,[14] but such is not the case.[9,30] Azkarate and Pelayo tested smooth tensile specimens of STA Beta C (σ_{YS} = 1250 MPa) under rising displacement in neutral NaCl at free corrosion, -1000 and -1500 mV_{SCE}.[16] STA Beta C was immune to EAC for the conditions examined, but Ti-6-4 (σ_{YS} = 1000 MPa) exhibited EAC at -1500 mV_{SCE}. Wolfe *et. al.* reported that smooth tensile specimens of STA Beta C (σ_{YS} = 1100 MPa) were immune to EAC in seawater with cathodic protection.[15] Comparison of these results to the data in Figs. 5 and 6 attests to the importance of an occluded crack to promote EAC.

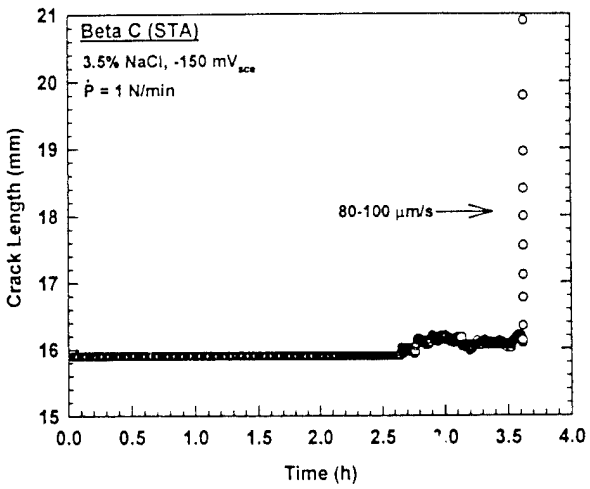

Figure 10. Crack length versus time for a constant loading rate of 1 N/min. (STA Beta C in 3.5% NaCl at -150 mV_{SCE}, K_{TH} = 44 MPa$\sqrt{m}$, da/dt = 80 to 100 μm/s.)

Limited studies with statically loaded precracked specimens showed that STA Beta C is immune to EAC. Thomas and Seagle did not produce brittle cracking in precracked C-rings in NaCl at several electrode potentials.[13] (EAC was produced by this method when H_2S was added to the environment and specimens were polarized cathodically.) Early studies with statically loaded precracked cantilever beam specimens of Beta C in aqueous chloride demonstrated similar immunity to EAC, however, low plane strain fracture toughness clouded the results.[17,18] Comparison of these findings to the data in Figs. 5, 6 and 7 attests to the importance of active loading to promote EAC of Beta C.

The experimental results for intergranular EAC of STA Beta C, showing the deleterious effects of the fatigue crack plus active loading and electrode potentials near free corrosion levels, are identical to data obtained for STA Beta 21S.[8,28]

Comparison of EAC in β Titanium Alloys and Ferritic Steels

Figure 11 summarizes K_{TH} and K_{IC} versus σ_{YS} results for Beta C in chloride solutions, compared to data for STA Beta 21S and STA Ti-15-3,[8] and superimposed with EAC K_{TH} for ferritic and martensitic steels in a variety

of hydrogen-producing gases and electrolytes.[11]2 The large shaded band shows the range of K_{TH} results, with upper (UB) and lower (LB) bounds on extensive threshold data for many steels in neutral chloride at free corrosion. (The open diamond shows a single K_{TH} result for moderate strength HY130 steel in NaCl, obtained with a single-edge-crack specimen and the fracture mechanics method used in the current study.)

For steels, it is well established that K_{TH} for hydrogen environment embrittlement decreases with increasing σ_{YS}.[11,31] For the ß-titanium alloys, plane strain fracture toughness decreases with increasing σ_{YS} (small filled circles), with a single trend observed for Beta C and Ti-15-3 and a higher strength-toughness trend seen for Beta 21S. K_{TH} values for STA Ti-15-3 (large open circles) and ST Beta C (large filled circles at σ_{YS} of 850 MPa) in NaCl essentially equal the K_{IC}-σ_{YS} trend line, indicating immunity to EAC. The results for ST Beta C (large filled circles) and STA Beta C (open squares) suggest a strength effect on K_{TH} that is similar to the trend for steels in neutral chloride. Alloy microstructure may play a critical role in determining the EAC resistance of ß-titanium alloys. The relative contributions of microstructure and yield strength in governing the EAC resistance of ST Beta C and the susceptibility of STA Beta C are not defined.

Intergranular EAC and Microstructure of ß-Titanium Alloys

An analysis of STA Beta 21S and Ti-15-3 correlated intergranular chloride EAC with microstructure, particularly α colonies precipitated at ß grain boundaries and/or intense slip localization.[8,28,32]

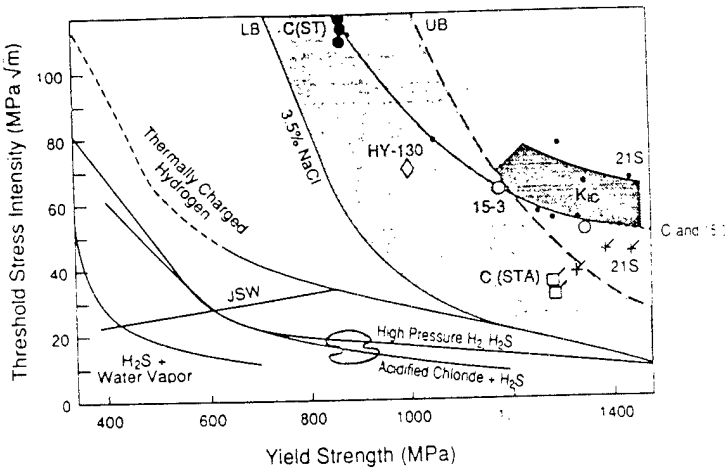

Figure 11. K_{TH} versus σ_{YS} for steels[11] and selected β-Ti alloys in chloride and other hydrogen-producing environments including sulfur-species additions.

---

[2]Hydrogen-producing environments are capable of generating atomic hydrogen on strain-cleaned crack tip surfaces by cathodic proton or water reduction for aqueous electrolytes, by dissociative chemical adsorption for H_2, or by chemical reaction for H_2S or H_2O gases. This hydrogen is available to embrittle metal within the crack tip process zone.[31]

EAC-prone Beta 21S exhibited both microstructural features, but EAC-resistant Ti-15-3 did not. Both microstructural features, as well as EAC and internal hydrogen embrittlement, appear to be promoted by prolonged solution treatment (in excess of 1 hour) at high temperature (above 950°C).

Beta C, solution treated in the EAC-resistant regime of relatively shorter time and lower temperature, exhibited an α-precipitate distribution and slip morphology between that of Beta 21S and Ti-15-3. While STA microstructures are complex, heat treatment experiments indicated that grain boundary α-colonies are less frequent in STA Beta C,[33] compared to both the microstructure of STA Beta 21S[8] and the amount of intergranular EAC shown in Fig. 6. These preliminary microstructural results, and the low solution treatment time and temperature, are inconsistent with a correlation between large α-colonies at ß grain boundaries and intergranular EAC in Beta C. Work is in progress to better address this issue.

Considering slip morphology, compression experiments showed that plastic deformation in ST Beta C is qualitatively homogeneous, with some grains deforming by locally intense slip bands.[33] Upon aging to the STA condition, slip band spacing decreases, and bands appear more planar and likely to cross entire grains. Similar locally planar deformation modes are observed for STA Beta C and Beta 21S, compared to homogeneous deformation in STA Ti-15-3.[8,32-35] This comparison suggests that slip localization plays a role in the intergranular chloride EAC of ST and STA ß titanium alloys, however, additional research is required.

The present results for Beta C show that high solution treatment temperature and/or prolonged time are not the sole requisite for intergranular EAC in ß titanium alloys. Interactions between yield strength and microstructure, or additional microstructural effects such as grain boundary impurity segregation,[36] must be considered.

Sulfur-Species Additions

Figure 11 shows that acidified chloride/H_2S solution at 25°C severely decreases the threshold for EAC of ferritic steels from that of aqueous chloride alone. Also shown in Fig. 11 are the data for ST Beta C in neutral NaCl and the acidified chloride/sulfur compound solutions summarized in Table I (large filled circle symbols plotted from Fig. 3). Notably for Beta C, K_{TH} did not decrease for any of the sulfur-bearing solutions, even acidified (pH 1.3) NaCl with Na_2S which formed H_2S. This sulfide-EAC resistance of ST Beta C is striking. For steels at a similar yield strength, acidified chloride and H_2S decrease K_{TH} to values as low as 15 MPa√m. K_{TH} for ST Beta C in the various sulfur-species-bearing electrolytes is about 5-fold higher than this lower limit and equals K_{IC}.

The sulfide EAC resistance of ST Beta C may be reduced by long term exposure that allows bulk specimen hydrogen uptake from boldly exposed surfaces. The short term-rising displacement experiments employed to obtain the data in Fig. 3 involved 24 hour exposures to the solution and were designed to emphasize crack dissolution and hydrogen production. Given a typical hydrogen diffusivity (D_H) in single phase ß titanium alloys of 4 x 10^{-7} cm^2/sec or faster,[32] about 12 hours are required for substantial hydrogen penetration from the root of the side-groove to the center line of the CT specimen, parallel to the crack front. If D_H is slower for ST Beta C or if reactions involving sulfide are relatively slow-building then longer exposure times could result in lower K_{TH} based on a hydrogen embrittlement scenario.[11,13,28] This issue must be investigated for cases where ST ß-titanium alloys encounter sulfide in an electrolyte, for example, as produced by sulfate-reducing bacteria in marine environments.[37]

Potentiostatic Polarization and K_{TH} for EAC

The threshold for chloride EAC in STA Beta C depends on applied electrode potential. This alloy was immune to EAC under cathodic polarization to -1000 mV_{SCE}, showed a minimum resistance (K_{TH}) at -600 mV_{SCE}, and was somewhat less cracking-prone with increasing potential at -150 mV_{SCE} (Fig. 8). The beneficial effect of cathodic polarization was reported by others for α/ß and ß/α titanium alloys in halogenated electrolytes.[2-5,38] In particular Young *et. al.*[8] reported that the neutral chloride K_{TH} for STA Beta 21S increased to equal K_{IC} when the specimen was polarized cathodically to -1000 mV_{SCE}, Fig. 8. Similar low K_{TH} values were observed at -600 and -150 mV_{SCE}, without evidence of a minimum EAC resistance. A speculative hydrogen environment embrittlement mechanism, focusing on atomic hydrogen production and uptake at the occluded and strain-hardened crack tip, was proposed to explain the electrode potential dependence shown in Fig. 8.[8]

The chloride EAC resistance of STA Beta C, under cathodic polarization, may be reduced by long term exposures that allow bulk specimen hydrogen uptake from boldly exposed specimen surfaces. That is, hydrogen may be produced on such surfaces, even if crack tip production and uptake are minimized by cathodic polarization.[39]

Implications of Slow-Rapid EAC Growth Rates

Alternating slow-rapid subcritical crack propagation could be explained mechanistically; hydrogen from cathodic reaction diffuses ahead of the crack tip, embrittles the process zone, and the crack rapidly propagates until arrest by surrounding non-embrittled material.[28] For STA

Beta C in NaCl, rapid EAC propagation occurs over distances that are much larger than the crack tip process or plastic zone (Fig. 9), transitions in the fracture surface morphology are not observed by SEM, and oscillating crack growth kinetics are not evident under rising load control. Thus, the slow-rapid da/dt phenomenon is not ascribed to time-dependent hydrogen diffusion.

Meyn and Pao observed oscillating subcritical crack growth kinetics for α/β Ti-6-4 and perhaps β/α STA Ti-15-3 in neutral aqueous NaCl during slow constant extension rate experiments.[40] At higher extension rates, continuous Stage II EAC occurred. It was proposed that a critical crack tip strain rate was necessary to maintain conditions conducive to Stage II crack growth. Webb and Meyn recently developed a crack driving force *vs* resistance model of oscillating EAC da/dt, based on assumed da/dt *vs* strain energy release rate (*G*) dependencies, and including test system compliance.[41] While they do not provide a mechanistic explanation for the form of da/dt *vs* *G* necessary to produce slow-rapid da/dt during rising displacement loading, they suggest that titanium alloy/environment systems exhibiting Stage IIA-Stage II subcritical crack growth kinetics are unique candidates for oscillations. Oscillating crack growth kinetics are expected to yield a sawtooth K-Δa curve, where the minimum and maximum K levels are constant. Measured minimum and maximum K levels for STA Beta C/NaCl in Fig. 9 are not constant.

Classically, subcritical EAC da/dt is measured and modeled based on either K-control or crack tip strain rate ($\dot{\epsilon}_{CT}$)-control.[11,42] Rather, for titanium alloys in chloride, we propose that da/dt depends interactively on both K and $\dot{\epsilon}_{CT}$, with steep near-threshold regimes for both variables. This hypothesis is based on the notion that K governs the crack tip process zone, relevant to hydrogen embrittlement, while $\dot{\epsilon}_{CT}$ governs the extent of crack surface electrochemical reactions, pertinent to hydrogen production, or process zone dislocation transport. The slow-rapid crack growth behavior shown in Fig. 9 is then controlled by specimen compliance-based changes in K and $\dot{\epsilon}_{CT}$ for the experiments conducted in rising-CMOD control. Note that da/dt is not a unique function of K for STA Beta C. For example, both slow and rapid da/dt are observed at a K level of 40 MPa$\sqrt{m}$.

Determination of the three-dimensional relationship between da/dt, K and $\dot{\epsilon}_{CT}$ is complicated by uncertainties in the calculation of crack tip strain rate. For a propagating crack, this quantity depends on K, dK/dt and da/dt, however, the precise function is clouded by uncertain parameters in the continuum mechanics formulation,[43,44] and by the role of localized dislocation processes. None-the-less, a continuum estimate of the crack tip opening displacement rate (δ_T),[43,44] which may be proportional to $\dot{\epsilon}_{CT}$, shows

that δ_T at the onset of rapid crack propagation is at least an order of magnitude less than that at the point where rapid da/dt begins to arrest. This estimate indicates that da/dt must be controlled by the interaction of K and $\dot{\epsilon}_{CT}$. Experiments and additional analyses are required to test the relative contributions of stress intensity and crack tip strain rate, and to determine the extent to which slow-fast da/dt behavior is unique to titanium alloys in environments that form a passive film at the crack tip.

CONCLUSIONS

1. The high-strength ß/α titanium alloy, STA Beta C, is embrittled by loading in neutral aqueous NaCl solution at 25°C, given an occluded crack, active strain rate and electrode potentials near free corrosion. This behavior is analogous to that of STA Beta 21S.

2. STA Beta C resists crack propagation in NaCl under static load/displacement or cathodic polarization, at least for short-term experiments. This behavior is analogous to that of STA Beta 21S.

3. Moderate strength, single phase (ß) ST Beta C is immune to chloride EAC at the free corrosion potential and under short-term rising displacement. Sulfur-species and acid additions to NaCl that embrittle ferritic steels do not promote intergranular EAC in ST Beta C.

4. EAC in STA Beta C is intergranular; the contributions of grain boundary α precipitation, locally intense planar slip and impurity segregation are not defined. Moist air fracture of the STA and ST conditions, as well as ST fracture in chloride-sulfur-species solutions, are by transgranular microvoid rupture.

5. The rising CMOD method is effective, but requires instrumentation and analysis of da/dt as a function of K and crack tip strain rate.

6. Alternating slow-rapid EAC propagation rate is speculatively attributed to coupled K- and crack tip strain rate-control, and specimen compliance-induced changes in these driving force parameters.

ACKNOWLEDGEMENTS

This research was supported by the Office of Naval Research (Grant N00014-91-J-4164), with A. John Sedriks as Scientific Monitor and a National Science Foundation Graduate Research Fellowship (for JAG). Material was donated by RMI Titanium Company and R.W. Schutz. These contributions are gratefully acknowledged, as are informative discussions with J.R. Scully, R.G. Kelly, M.A. Gaudett, and D.G. Kolman.

REFERENCES

1. R.W. Schutz, JOM, vol. 46, no. 7, 1994, pp. 24-29.
2. R.W. Schutz and D.E. Thomas, in Metals Handbook: Corrosion, vol. 13, 9th ed., ASM Int'l, Materials Park, OH, 1987, pp. 669-706.
3. M.J. Blackburn, J.A. Feeney, and T.R. Beck, in Advances in Corrosion Science and Technology, M.G. Fontana and R.W. Staehle, eds., vol. 3, Plenum Publishing, NY, NY, 1972, pp. 67-292.
4. R.W. Schutz, in Stress Corrosion Cracking, R.H. Jones, ed., ASM Int'l, Materials Park, OH, 1992, pp. 265-297.
5. M.J. Blackburn, W.H. Smyrl, and J.A. Feeney, in Stress Corrosion Cracking in High Strength Steel and in Titanium and Aluminum Alloys, B.F. Brown, ed., Naval Research Laboratory, Washington, DC, 1972, pp. 245-363.
6. J.A. Moskovitz and R.M. Pelloux, Corrosion, vol. 35, 1979, pp. 509-514.
7. J.A. Feeney and M.J. Blackburn, Met. Trans., vol. 1, 1970, pp. 3309-3323.
8. L.M. Young, G.A. Young, Jr., J.R. Scully, and R.P. Gangloff, Metall. Mater. Trans. A, in review, 1994.
9. B.F. Brown, Mater. Res. Std., 1966, vol. 6, pp. 129-136.
10. D.N. Fager and W.F. Spurr, Trans. ASM, vol. 61, 1968, pp. 283-292.
11. R.P. Gangloff, in Corrosion Prevention and Control, M. Levy and S. Isserow, eds., US Army Laboratory Command, Watertown, MA, 1986, pp. 64-111.
12. Atlas of Stress-Corrosion and Corrosion Fatigue Curves, A.J. McEvily, Jr., ed., ASM Int'l, Materials Park, OH, 1990, pp. 457, 484.
13. D.E. Thomas and S.R. Seagle in Titanium Science and Technology, G. Lutjering, U. Zwicker and W. Bunk, eds., 1984, pp. 2533-2540.
14. D.M. Aylor, "An Environmental Cracking Evaluation of Fastener Materials for Seawater Applications" (paper No. 484 presented at NACE Corrosion '94, Houston, TX, 1994).
15. L.H. Wolfe, *et al.*, Materials Performance, vol. 32, no.7, 1993, pp. 14-21.
16. I. Azkarate and A. Pelayo, "Hydrogen Assisted Stress Cracking of Titanium Alloys in Aqueous Chloride Environments" (paper presented at INASMET, San Sebastian, Spain, 1992).
17. W.F. Czyrklis and M. Levy, Corrosion, vol. 32, 1976, pp. 99-102
18. J.W. Hagemeyer and D.E. Gordon, in Titanium Science and Technology, Plenum Press, New York, NY, 1973, pp. 1957-1968.
19. B.P. Somerday, Y. Leng, and R.P. Gangloff, Fatigue and Fracture of Engineering Materials and Structures, in review, 1994.

20. Annual Book of ASTM Standards, Designation E1152-87, vol. 3.01, ASTM, Philadelphia, PA, 1989, pp. 814-824.
21. R.A. Mayville, T.J. Warren, and P.D. Hilton, Trans. ASME, vol. 109, 1987, pp. 188-193.
22. J.K. Donald and J. Ruschau, in Fatigue Crack Measurement: Techniques and Applications, K.J. Marsh *et al.*, eds., EMAS, West Midlands, UK, 1991, pp. 11-37.
23. J.K. Gregory and L. Wagner, "Heat Treatment and Mechanical Behavior in Beta C" (paper presented at GTT, Torino, Italy, 1991).
24. S. Mat and R.C. Newman, "Local Chemistry Aspects of Hydrogen Sulfide-Assisted Stress Corrosion Cracking of Stainless Steels" (paper No. 228 presented at NACE Corrosion '94, Houston, TX, 1994).
25. J.R. Scully and P.J. Moran, Corrosion, vol. 44, 1988, pp. 176-185.
26. S. Tsujikawa *et al.*, Corrosion, vol. 49, 1993, pp. 409-419.
27. H.H. Uhlig, Materials Performance, vol. 16, no. 1, 1977, pp. 22-25.
28. L.M. Young, *Environment-Assisted Cracking in Beta Titanium Alloys*, MS Thesis, University of Virginia, Charlottesville, VA, 1993.
29. H.B. Bomberger, D.A. Meyn and A.C. Fraker, in Titanium Science and Technology, G. Lütjering, U. Zwicker and W. Bunk, eds., Deutsche Gesellschaft für Metallkunde e.V., Obserusel, West Germany, 1985, pp. 2435-2454.
30. H. Buhl, in Stress Corrosion Cracking-The Slow Strain Rate Technique, ASTM STP 665, G.M. Ugiansky and J.H. Payer, eds., ASTM, Philadelphia, PA, 1979, pp. 333-346.
31. R.P. Gangloff, Matls. Sci. Engr. A, vol. 103, 1988, pp. 157-166.
32. G.A. Young, Jr., *Hydrogen Effects in Metastable β-Titanium Alloys*, M.S. Thesis, University of Virginia, Charlottesville, VA, 1993.
33. M.A. Gaudett and J.R. Scully, unpublished research, University of Virginia, Charlottesville, VA, 1994.
34. G.A. Young, Jr. and J.R. Scully, Scripta Metall., vol. 28, 1993, pp. 507-512.
35. G.A. Young, Jr. and J.R. Scully, in Beta Titanium Alloys in the 1990s, D. Eylon, R.R. Boyer and D.A. Koss, eds., TMS-AIME, Warrendale, PA, 1993, pp. 147-158.
36. H.J. Rack, Metall. Trans. A, vol. 6A, 1975, pp. 947-949.
37. R.P. Gangloff and R.G. Kelly, Corrosion, vol. 50, 1994, pp. 345-354.
38. T.R. B k, J. Electrohem. Soc., vol. 114, 1967, pp. 551-556.
39. A. Turnbull. Scripta Metall., vol. 20, 1986, pp. 365-369.
40. D.A. Meyn and P.S. Pao, in Slow Stain Rate Testing for the Evaluation of Environmentally Induced Cracking: Research and Engineering Applications, ASTM STP 1210, R.D. Kane, ed., ASTM, Philadelphia, PA, 1993, pp. 158-169.
41. T.W. Webb and D.A. Meyn, Fracture Mechanics 26th Volume, ASTM STP 1256, W.G. Reuter, J.H. Underwood and J.C. Newman, Jr., eds., ASTM, Philadelphia, PA, in review, 1994.
42. F.P. Ford, in Environment Induced Cracking of Metals, R.P. Gangloff and M.B. Ives, eds., NACE, Houston, TX, 1990, pp. 139-166.
43. J.R. Rice, W.J. Drugan and T-L. Sham, in Fracture Mechanics: 12th Conference, ASTM STP 700, ASTM, Philadelphia, PA, 1980, pp. 189-221.
44. J.R. Rice and E.P. Sorensen, J. Mech. Phys. Solids, vol. 26, 1978, pp. 163-186.